

Transient photomodulation spectroscopy of nanocrystalline hydrogenated silicon

Lingrong Chen and J. Tauc

Division of Engineering and Department of Physics, Brown University, Providence, Rhode Island 02912

Z. Vardeny

Department of Physics, University of Utah, Salt Lake City, Utah 84112

(Received 4 August 1988)

Transient photomodulation spectra were measured on nanocrystalline Si:H films in the time domain from 10^{-7} to 10^{-2} s, spectral range from 0.25 to 1.25 eV, and temperature range from 80 to 300 K. The properties of the spectra are compatible with the presence of two phases, amorphous and crystalline. The amorphous phase is similar to *a*-Si:H. Photoinduced free-carrier absorption is associated with the crystalline phase; its decay is described by a stretched exponential which extends into much longer times than the exponential decays in crystalline Si. A model for the recombination process is proposed.

INTRODUCTION

Thin films of Si prepared by chemical transport in low-pressure hydrogen plasma at temperatures below 300°C have been shown to be composed of crystallites whose sizes are in the range 50–1000 Å depending on the conditions during the deposition.¹ The material interconnecting the crystallites is highly disordered; its properties vary with the preparation conditions.² This kind of Si film was originally referred to as “microcrystalline” hydrogenated Si; later, the term “nanocrystalline” (nc-Si:H) was introduced, which we use in this paper. We will refer to the intergrain materials as the “amorphous phase.” It is not obvious that a simple division into crystalline and amorphous phases is always possible;^{2,3} we will show how well our data support it.

There has recently been increased interest in the properties of clusters, and nc-Si:H is an interesting material from this point of view. An additional justification for studying nc-Si is its importance for devices.⁴ This material can be much more heavily doped with donors or acceptors than *a*-Si:H, while, similar to *a*-Si:H, the optical absorption in the visible range is much higher than in *c*-Si.^{5,6}

In this paper, we report on time-resolved photomodulation (PM) studies in nc-Si:H. In the previous study⁷ of steady-state PM, free-carrier contribution was identified and studied. This study of the transient PM spectra, measured in broad time, temperature, and pump-intensity ranges, provides information about the time-resolved photocarrier distributions, their trapping, and their recombination, which in turn leads to information about the transport of carriers between the two phases, about the band tails and defects in the amorphous matrix, and additional information about carriers in the crystalline phase.

EXPERIMENTAL

The PM spectroscopy requires two light sources: a pump beam for photogeneration of carriers, and a probe

beam for measuring the photoinduced changes in transmission. For the steady-state measurements the pump was a mechanically chopped (75 Hz) Ar⁺ laser beam with an intensity of 100 mW/cm² and the probe beam was derived from an incandescent lamp dispersed by a monochromator. The transmission *T* and its modulation ΔT were recorded in the spectral range of 0.25–1.8 eV. The transient measurements were done using the system developed by Stoddart.^{8,9} The pump pulse source was a Nd:YAG (YAG denotes yttrium aluminum garnet) laser with a frequency doubler. The pulse duration was about 10 ns, the energy per pulse was 100 μ J, the repetition rate was 20 s⁻¹, and the diameter of the illuminated spot was about 1 cm. The probe beam was produced by an incandescent lamp whose light was spectrally resolved using a set of interference filters of known transmission characteristics;⁸ they covered a range 0.2–1.8 eV with an approximate resolution of 0.1 eV. The spectra were recorded using two signal averagers and a computer for the time range 300 ns–30 ms. The data are presented in the form of $\Delta T/T$. In *a*-Si:H, photoinduced changes in reflectivity can be neglected below 1.8 eV;¹⁰ in this case $-\Delta T/T = d \Delta\alpha$, where *d* is the film thickness (if $d < \alpha^{-1}$), or, if $d > \alpha^{-1}$, $-\Delta T/T = \Delta\alpha/\alpha$, where $\Delta\alpha$ is the change in the absorption coefficient α .

The samples were films 3–5 μ m thick on crystalline Si substrates. They were prepared by the glow-discharge process in low-pressure hydrogen plasma in the floating potential condition by the amorphous semiconductors group at Nanjing University. The substrate was held at 300°C. Different average grain sizes in the range from 30 to 830 Å were obtained by varying the rf power from 13 to 145 W (the current varied from 70 to 300 mA). The Nanjing group determined the average grain sizes of the samples using two methods.¹¹ For sizes smaller than 400 Å the width of the x-ray diffraction peak corresponding to the [111] direction was measured; for larger sizes the scanning electron microscope was used. We checked these measurements using the Raman method proposed by Iqbal and Vepřek.¹² We measured the position of the

TO Raman line excited with the 514.5-nm line of an Ar^+ laser in a backscattering configuration using a three-grating monochromator. The system was calibrated by using the TO Raman line of (111) face of a single-crystal Si (520 cm^{-1}). The corresponding peaks in the Raman spectra of nc-Si:H samples are shifted towards smaller energies as the average grain size decreases. The Raman spectra of our samples give the same ordering of the sizes as the Nanjing group's ordering. The Raman method is not applicable for quantitative determination of grain sizes exceeding 150 \AA .¹² However, for our smallest size sample (sample *B*) the TO phonon Raman peak is at 518 cm^{-1} , which, according to Iqbal and Vepřek,¹² corresponds to the average grain size of 80 \AA ; the size given by the Nanjing group is 70 \AA .

RESULTS

Steady-state PM spectra of three films with crystallite grain size of 830 \AA (sample *D*), 420 \AA (sample *C*), and 70 \AA (sample *B*) at temperature $\Theta = 150\text{ K}$ are shown in Fig. 1. We note that the spectrum of sample *B* is similar to the PM spectrum observed in undoped *a*-Si:H.¹³ It is characterized by a PM band with an onset of photoinduced absorption (PA) at about 0.5 eV followed by photoinduced bleaching (PB) at about 1.0 eV . The spectrum of sample *D* is very different. The PM band is weak and the dominant feature is the strong onset of absorption at low energies; from its characteristics to be discussed below (see also Ref. 7) we will refer to it as photoinduced free-carrier absorption (PFCA). The spectrum of sample *C* shows both characteristics of samples *B* and *D*; with respect to sample *B*, the PA band is shifted towards higher energies.

The dependence of ΔT on the pump intensity is sub-linear, $-\Delta T \sim I^\eta$, with $\eta = 0.5 \pm 0.15$. η depends little on temperature and probe wavelength. The temperature (Θ) dependence of the PM spectra of sample *C* is shown in Fig. 2. We note that the PFCA decreases more quickly with temperature than the PM band. This is clearly seen in Fig. 3, where the temperature dependence of the PA strength in sample *D* at two energies, 0.25 and 0.75 eV , is

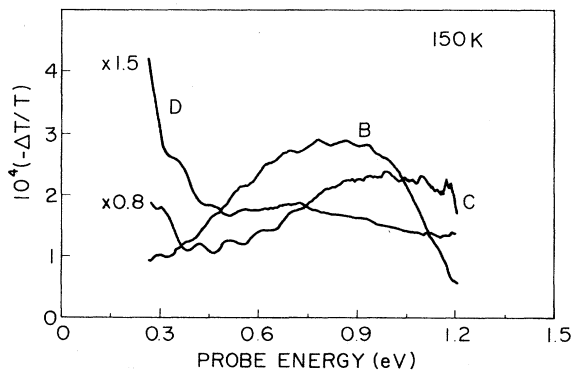


FIG. 1. Steady-state PM spectra of three samples—*D*, *C*, and *B*—at 150 K : grain sizes are 830 \AA (sample *D*), 420 \AA (sample *C*), and 70 \AA (sample *B*).

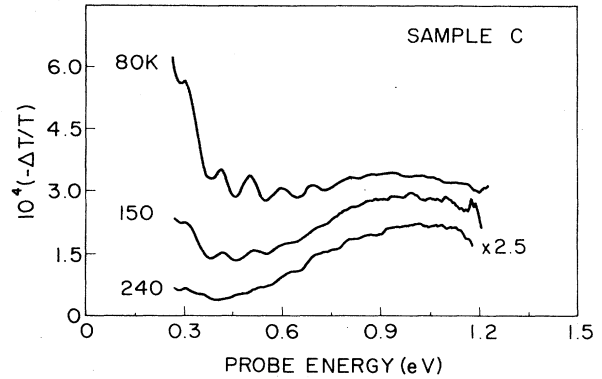


FIG. 2. Temperature dependence of the steady-state PM spectra of sample *C*.

shown. The temperature dependence is exponential, $-\Delta T/T \sim \exp(-\Theta/\Theta_0)$, where $\Theta_0 = 157\text{ K}$ at 0.25 eV and $\Theta_0 = 337\text{ K}$ at 0.75 eV . This result confirms the assumption that there are two different contributions to the PM spectrum of nc-Si:H. At 0.25 eV , PFCA prevails, while at 0.75 eV the PM band characteristic of *a*-Si:H prevails. The reasons why long-wavelength photoinduced absorption is ascribed to free carriers were discussed in Ref. 7. The strongest argument is the wavelength dependence which is proportional to λ^δ , where δ is in the range of 1.7 – 1.8 for samples *D* and *C*, nearly independent of the grain size and temperature.

Figure 4 shows two examples of transient PM spectra measured at different times after pulse excitation (sample *D* at 80 and 300 K). The transient spectra were constructed from a series of PM decays measured at different probe photon energies, similar to those in Refs. 8 and 9. The data shown here include the theoretical curves which will be discussed later on. The strength of the spectra and their shape strongly depend on time and tempera-

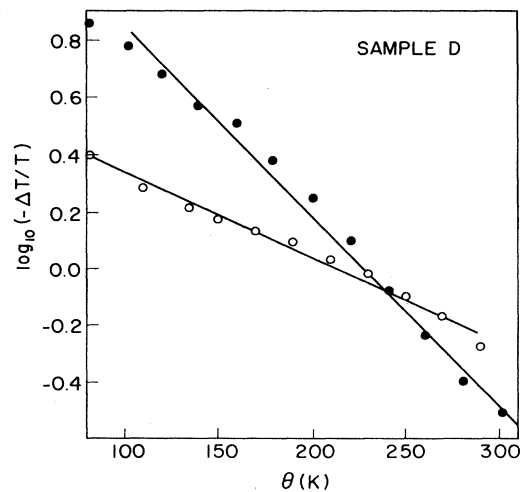


FIG. 3. Temperature dependencies of steady-state PM spectrum in sample *D* at the probe energies of 0.25 and 0.75 eV .

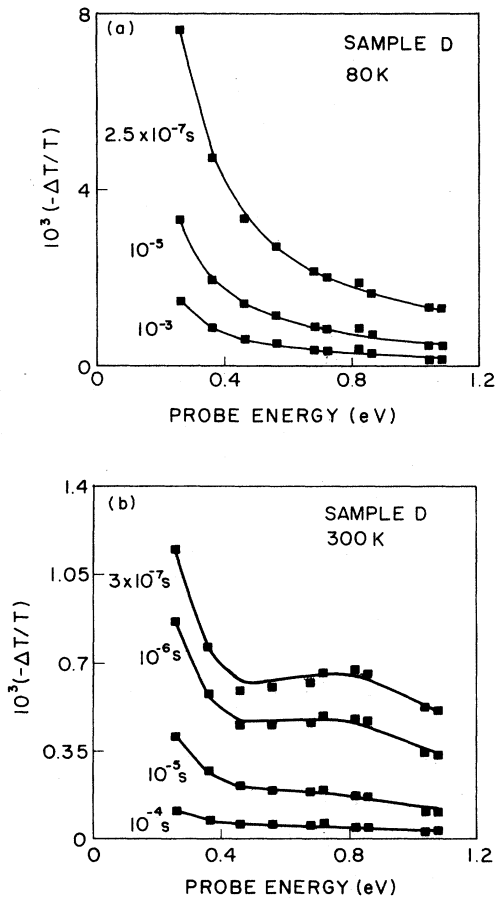


FIG. 4. (a) Transient PM spectra of sample *D* measured at 80 K at time delays of 2.5×10^{-7} , 10^{-5} , and 10^{-3} s. The points are the data, the curves are theoretical fits. (b) Data and fitting at 300 K.

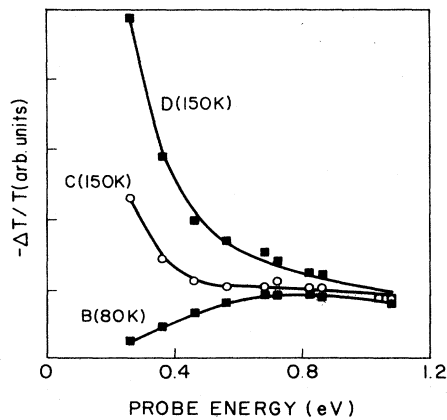


FIG. 5. Comparison of measured PM spectra and theoretical fits at 150 K and a time delay of 10^{-5} s for three samples—*D*, *C*, and *B*.

ture. The transient spectra of samples *B*, *C*, and *D*, measured at $10 \mu\text{s}$, are compared in Fig. 5. The temperature was 150 K except for sample *B* whose signal was too low at 150 K and the data shown are at 80 K. We note that these spectra and their temperature dependencies are similar to the steady-state spectra (Fig. 1). The time dependencies will be discussed later.

ANALYSIS OF THE TRANSIENT SPECTRA

For describing the transient spectra, we assumed that there are contributions from photoinduced free carriers (FC's) associated with the crystalline phase and from transitions involving the states deep in the gap and the band tails in the amorphous phase (PM bands). For PFCA we used a power-law function $\Delta\alpha = A(t)(\hbar\omega)^{-\delta}$, where $A(t)$ and δ are adjustable parameters. For the PM bands in the *a*-Si:H phase we used the same model as previously used for *a*-Si:H.^{8,9} At high temperatures, the PM band is associated with the dangling bonds (DB's) which are neutral in the dark (D^0); they become charged (D^+ , D^-) by trapping photocarriers. Since only one PM band is observed, the energies of D^+ and D^- have to be symmetrically displaced¹³ from the midgap by energies $-E_{\text{DB}}$ and $+E_{\text{DB}}$ (DB denotes dangling bond). The state distribution of D^+ , D^- is assumed to be a Gaussian with a width ΔE_{DB} . The photoinduced $\Delta\alpha$ is proportional to the convolution of this distribution with the density of the continuum band, which is assumed to be proportional to $(E - E_b)^{1/2}$ (E_b is the band edge). The matrix element is assumed to be constant. There are two contributions associated with DB's—PA and PB (Ref. 13)—whose amplitudes C_a and C_b are adjustable parameters.

The PM band is dominated by transitions involving the DB's at high temperatures,¹³ but at low temperatures the contributions associated with the transitions from the band tail (BT) into the adjacent band are important. Again we follow the work of Stoddart *et al.*^{8,9} for the description of these transitions. For reasons that are not well understood, in *a*-Si:H only hole transitions into the valence band are observed. We used the square-root energy distribution for the continuum band, which we convoluted with the transient distribution of carriers (as calculated in Refs. 8 and 9) in the band tail, whose state density is assumed to be an exponential with a width E_0 . The BT contribution to the PM is characterized by an amplitude $B(t)$ and the BT width E_0 (time independent) and by the demarcation energy $E_d(t)$ (E_d is defined as the energy separating those states which already have released the carriers and those which have not done so at time t).¹⁴ The transient spectra at each temperature in the time range of 10^{-7} – 10^{-2} s (altogether about 200 spectra) were simultaneously fitted using six fixed parameters (δ , E_0 , C_a/C_b , E_{DB} , E_g , and ΔE_{DB}) (E_g is the gap) for each grain size and four time-dependent parameters [$A(t)$, $B(t)$, $C_a(t)$, and $E_d(t)$]. Examples of the fits are shown in Figs. 4 and 5; they were obtained with the following fixed parameters: $\delta = 1.75(\pm 0.1)$, $E_0 = 58$ meV, $C_a/C_b = 10/7$, $E_{\text{DB}} = 0.2$ eV, $E_g = 1.4 \pm 0.05$ eV, and $\Delta E_{\text{DB}} = 0.27 \pm 0.03$ eV. The time-dependent parameters $A(t)$, $B(t)$, and $C_a(t)$ describing the strengths of the

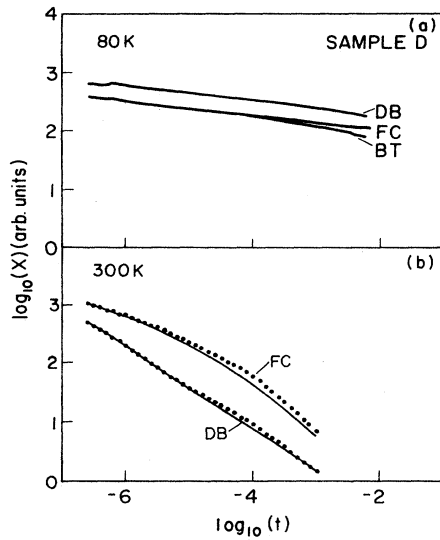


FIG. 6. (a) Comparison of the decay of transitions associated with the free carriers (FC's), band-tail (BT) states, and dangling bonds (DB's) at 80 K for sample *D* [functions $A(t)$, $B(t)$, and $C_a(t)$, respectively, as used in the text]. (b) The dotted curves represent $A(t)$ and $C_a(t)$ at 300 K, obtained by the same procedures as in (a). The solid curve labeled FC is the curve for 300 K in Fig. 8; the derivative of its logarithm is the solid curve labeled DB.

different PM contributions [$A(t)$ for FC's, $B(t)$ for BT's, and $C_a(t) = (10/7)C_b(t)$ for DB's] at $\Theta = 80$ and 300 K for sample *D* obtained from the fitting are shown in Fig. 6(a) and 6(b); the curves are arbitrarily shifted relative to each other. At 80 K [Fig. 6(a)], there are contributions to PM from FC's, DB's, and BT's; at higher temperatures the BT contribution is negligibly small. We note that at 80 K the decays of the FC and DB contributions are similar; at 300 K [Fig. 6(b)] the FC part decreases faster

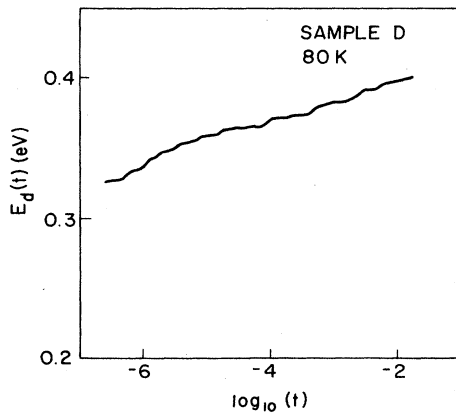


FIG. 7. The shift of the demarcation energy at 80 K in sample *D*.

than the DB band at long times. The shift of the demarcation energy $E_d(t)$ (measured from the band edge) with time as obtained from the fit at 80 K for sample *D* is shown in Fig. 7. The rate of the shift does not differ much from that observed in *a*-Si:H films at the same temperature, but the demarcation energy E_d is deeper than in *a*-SiH films.^{8,9}

FREE-CARRIER RECOMBINATION

We have studied in more detail the temperature dependence of the PFCA contribution to the PM spectrum in order to learn more about the recombination process of photogenerated carriers in the nanocrystalline phase. Rather than study the decay of $A(t)$ obtained by fitting the spectra [Figs. 6(a) and 6(b)], we directly obtained it from the measured PA at 0.25 eV. At this probe photon energy, PFCA is the dominant contribution for $\Theta > 150$ K; at lower temperatures, the BT contribution is not negligible and cannot be reliably separated. The results for sample *D* are shown in Fig. 8. The solid lines that fit the data so well in the time range 10^{-6} – 10^{-2} s were obtained using stretched exponentials,

$$-\Delta T/T = F \exp[-(t/\tau)^\gamma], \quad (1)$$

where F was found to be almost constant in the whole temperature range. The exponent γ and the recombination time τ are shown in Figs. 9(a) and 9(b) as a function of temperature (also for sample *C*). The accuracy of the fits with stretched exponentials can be judged from the master plot of Fig. 10, where we plot $\log_{10} F$ versus $\log_{10} |\Delta T/T|$ as a function of the stretched time $(t/\tau)^\gamma$ for the data obtained on sample *C* at three temperatures; neither simple exponentials nor power laws give useful fits.

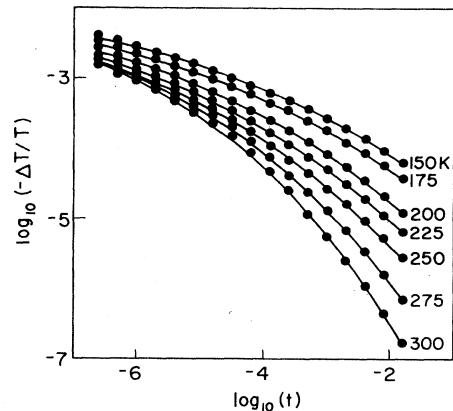


FIG. 8. Measured PFCA decays of sample *D* using a probe energy of 0.25 eV at several temperatures. The fits (solid lines) are stretched exponentials [Eq. (1)].

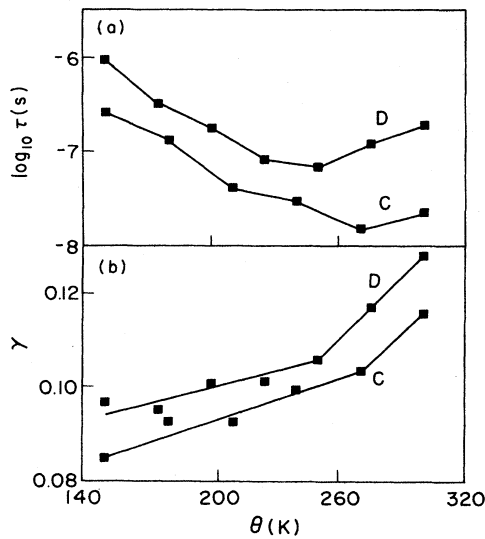


FIG. 9. (a) Temperature dependence of lifetime τ , obtained from fitting the stretched exponentials [Eq. (1)] observed in samples C and D. (b) Temperature dependence of the power index γ [Eq. (1)].

COMPARISON WITH CRYSTALLINE Si

Liu *et al.*⁷ have made an observation that in their steady-state measurements the PFCA in nc-Si:H was much stronger than in c-Si, and have suggested that this is due to a longer recombination time in the crystalline phase of nc-Si:H than in single-crystal Si. This is a strange proposition, because the nanocrystals are certainly more disordered, and crystal boundaries which usually have high combination rates are extremely close. It was suggested⁷ that the low recombination rate is due to a potential barrier between the nanocrystals and the amorphous phase which quickly separates the electrons and holes and reduces their chances of recombining. However, it is difficult to understand how effective barriers

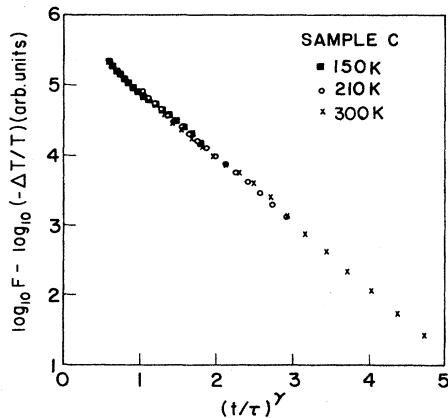


FIG. 10. Master plot of PFCA decays for sample C using data from measurements at three temperatures.

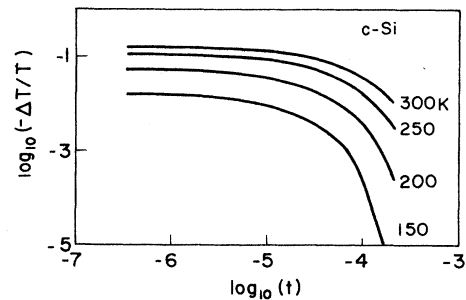


FIG. 11. Measured PFCA decays of high-quality single-crystal Si at different temperatures.

could be formed in the nanometer domain in a highly disordered material.

For shedding light on the question, we measured PA in crystalline Si under similar conditions as in nc-Si. In Fig. 11 we show the results obtained on a high-quality single-crystal Si using as a pump a Nd-YAG laser in the fundamental wavelength ($1.06 \mu\text{m}$) and a probe at 0.25 eV photon energy. The decays of PFCA are exponentials with recombination times in the range of 10–20 μs in the temperature range 80–300 K. These recombination times are longer than the values of τ found for nc-Si:H [Fig. 9(a)]. However, for $t > \tau$ the stretched exponentials with $\gamma < 1$ decay more slowly than the exponentials. Therefore, when one measures steady-state responses using chopping rates of less than 100 s^{-1} ($t \sim 10 \text{ ms}$), the signals in c-Si are very small, while the slow decays in nc-Si lead to much larger signals. From this point of view, the explanation of the observed differences in the strength of PA in c-Si and nc-Si:H is related to the origin of the stretched exponential; we will return to this point in the Discussion.

DISCUSSION

Amorphous phase

Although our results cannot definitely resolve the problem of whether two phases, crystalline and amorphous, are present in nc-Si:H, it is nevertheless remarkable how close some spectral features and time dependencies observed in nc-Si:H are to those found in a-Si:H.^{8,9} Both materials have similar PM bands that exhibit three components: band tail, dangling bonds D^\pm (associated with absorption), and D^0 (bleaching). The temperature dependencies of the PM band strengths in both materials obey the exponential law [$\sim \exp(-\Theta/\Theta_0)$]; at low Θ the PM at BT's prevails, while at high Θ the DB's dominate. The dependence on the pump intensity is similar in both materials ($\sim I^\eta$, where $\eta \sim 0.5-0.6$). Also, the correlation energies ($U_{\text{eff}} = 2E_{\text{DB}}$) of the DB defects are about the same¹³ ($\sim 0.4-0.5 \text{ eV}$).

There are also some differences between the amorphous phase in nc-Si:H and high-quality a-Si:H. As seen in Fig. 1, the PM peak in the steady-state spectra is at the same energy as in a-Si:H only for the smallest grain size (sample B); we do not understand the reasons for shifts in

samples *C* and *D* with larger grain sizes. In nc-Si:H the BT contribution is observable up to 150 K, while in *a*-Si:H it is observable up to 240 K. The demarcation energy $E_d(t)$ measured in sample *D* increases at about the same rate with t in nc-Si:H as in *a*-Si:H, but is deeper in nc-Si:H. These observations are compatible with a broader exponential distribution of states in the tail ($E_0=58$ meV in nc-Si:H and 46 meV in *a*-Si:H), indicating that the amorphous phase in nc-Si:H is more disordered than high-quality *a*-Si:H.

There is also a difference in the energies of the dangling bonds. For the transient PM in *a*-Si:H the onset of absorption associated with DB's is at 0.65 eV and the onset of bleaching at 1.1 eV; the corresponding numbers for nc-Si:H are around 0.5 and 0.9 eV (sample *D*) and 0.6 and 1.0 eV (sample *C*). If we assume that the gap E_g is the sum of these energies [as is the case in *a*-Si:H (Ref. 13)], then E_g is only 1.4 eV (sample *D*) and 1.6 eV (sample *C*) compared to 1.75 eV in *a*-Si:H. The smaller gap may also be related to the larger disorder. It is not possible to directly measure E_g of the amorphous phase in nc-Si:H to confirm this conclusion.

We may conclude that the properties of the PM spectra are compatible with a two-phase model. The amorphous phase has some similarities with *a*-Si:H, however, there are differences which can be understood as being due to increased disorder.

Recombination

The crystalline phase manifests itself in the spectral features associated with free carriers. We note that, to our knowledge, in the studied spectral range a free-carrier contribution has never been observed in *a*-Si:H. It therefore appears reasonable to assume that the PFCA occurs because of the presence of the crystalline phase; this is in agreement with x-ray diffraction data.¹¹ In the steady-state measurements reported previously⁷ it was observed that the PFCA signal was much stronger in nc-Si:H than in *c*-Si. A higher disorder in the nanocrystallites increases the PFCA but cannot explain a factor of 100 or more. In this work, this is directly confirmed by comparing the time-resolved PFCA in nc-Si (Fig. 8) and *c*-Si (Fig. 11). We see that at short times, under comparable conditions, the signal in *c*-Si is actually stronger than in nc-Si:H. Therefore the difference must be in the recombination. Our new data lead us to propose a somewhat more specific model about the recombination process than the previous model.⁷

Figure 6(a) shows that the induced absorption associated with BT, DB, and FC decays at low temperatures with the same rate. The decays of FC's and DB's are different at high temperatures as Fig. 6(b) shows (at 300 K the BT contribution is too weak to be measurable).

We cannot propose a definitive model, but we will discuss some plausible approaches to explain the observed facts. The aim is an understanding of why the recombination of free carriers which are in the crystalline phase has the characteristics associated with the amorphous phase, while the crystalline recombination process is not

observed at all. The following suggestions are based on the idea that the recombination rate in the crystal is strongly reduced because one of the carriers is preferentially trapped in the amorphous phase.

We will elaborate on this idea starting with the low-temperature results. The decays at 80 K follow the $t^{-\beta}$ power law with the same β for BT's, DB's, and FC's ($\beta=0.12$), which is close to the value of β in *a*-Si:H ($\beta=0.15$). This is an experimental fact, clearly indicating that the recombination in the amorphous phase determines the rate of recombination in the crystalline phase (FC's). We can only speculate why this happens and we will describe one possibility. The carriers photogenerated in the grains have high mobilities and reach the grain boundaries very quickly. Using the conclusions of the PA studies on *a*-Si:H,⁹ the existence of the BT contribution to PA shows that the holes are trapped in the valence band of the amorphous phase. To account for the observed PFCA we must assume that a large number of electrons stay behind in the grains. Their recombination is slower than in single-crystal Si because the hole density in the grain has been reduced by their trapping in the amorphous phase. It is necessary to assume that the electrons do not go from the grains into the conduction band or conduction-band-tail states of the amorphous phase, where the density of states is high and the mobilities are relatively large. A reason for this may be that the gap mismatch between the crystalline and amorphous phases introduces a barrier between these phases in the conduction band that prevents the electrons from entering the higher-lying states (presumably there is no such barrier between the valence bands that would prevent the motion of holes from the grains into the amorphous phase). However, the electrons can be trapped at the lower-lying D^0 states, converting them into D^- states. The recombination occurs between D^- and BT's (or D^+) similarly as in *a*-Si:H.⁹ The density of D^- states is low (compared to the BT densities), and at low T only a part of the DB states close to the grain may be accessible to the electrons from the grain; therefore, the density of the trapped electrons is smaller than that of the holes. Because of the high density of electrons in the grain, as D^- recombines ($D^- + h \rightarrow D^0$), the D^0 state captures relatively fast new electrons from the grain. Therefore, the disappearance of electrons in the grain is determined by the recombination rate in the amorphous phase.

We can explain the high-temperature data if we apply the same model but assume that the average mobility of electrons is much higher than at low temperature, presumably because the electrons can occupy higher energy states. Then the dominant recombination rate will be determined by how fast the electrons from the grain can reach a hole. At high Φ and long times ($t > 10^{-5}$ s) the density of holes trapped in the BT is small⁹ and most holes are in the D^+ states. We assume that we see those trapped holes as the DB band in our PM spectrum; its decay at 300 K is shown in Fig. 6(b).

Using this model, we can explain the stretched exponential decays found for the PFCA over a limited time range (Fig. 8) if we assume that the carrier's feeding rate into the grains is proportional to the density N_{DB} of D^+

states. In the equation for FC density n (electrons in the grain),

$$dn(t)/dt = -bn(t)N_{DB}(t) \quad (2)$$

we assume that the tunneling coefficient b is a constant. If $N_{DB}(t)$ [Fig. 6(b), dotted line labeled DB] decays within the accuracy of the data as a power law which we write as $N_{DB} \sim t^{-(1-\gamma)}$, then the integration of Eq. (2) gives the stretched exponential Eq. (1) as observed. We also checked this relation from the other side. According to Eq. (2), $d \ln n(t)/dt$ should be proportional to $N_{DB}(t)$. The solid line labeled DB in Fig. 6(b) is $d \ln n(t)/dt$ calculated from the data in Fig. 8; we see that it agrees reasonably well with the dotted line labeled DB which was obtained from the transient spectra fitting.

We may tentatively conclude that the existence of FCA proves the existence of a crystalline phase since in a -Si:H FCA has not been observed. This supports the two-phase model; the alternative would be a hypothetical phase with an arbitrary and unusual mixture of properties.

ACKNOWLEDGMENTS

We thank Yu-liang He, Shen Zongyong, and Yen Yionghong for preparing and characterizing the samples, M. Olszakier for the Raman measurements on the samples, and T. R. Kirst for technical assistance. The work at Brown University was partly supported by the National Science Foundation under Grant No. DMR-87-06289. We also acknowledge the use of the Optical Facility, partly supported by the Materials Research Laboratory program at Brown University.

¹Z. Iqbal, A. P. Webb, and S. Vepřek, *Appl. Phys. Lett.* **36**, 163 (1980).

²S. Vepřek, in *Proceedings of the Materials Research Society Symposium on Non-Crystalline Materials*, edited by P. Pinard and S. Kalbitzer (Les editions de physique, Les Ullis, France, 1984), p. 425.

³F. Boullitrop, A. Chenevas-Paul, and D. J. Dunstan, *Solid State Commun.* **48**, 181 (1983).

⁴K. Takahashi and M. Konagai, *Amorphous Silicon Solar Cells* (Wiley, New York, 1986).

⁵H. Richter and L. Ley, *J. Appl. Phys.* **52**, 7281 (1981).

⁶Z. Iqbal, F.-A. Sarott, and S. Vepřek, *J. Phys. C* **16**, 2005 (1983).

⁷Hsiang-na Liu, D. Pfost, and J. Tauc, *Solid State Commun.* **50**, 987 (1984).

⁸H. A. Stoddart, Ph.D. thesis, Brown University, 1987.

⁹H. A. Stoddart, Z. Vardeny, and J. Tauc, *Phys. Rev. B* **38**, 1362 (1988).

¹⁰H. T. Grahn, C. Thomsen, and J. Tauc, *Opt. Commun.* **58**, 226 (1986).

¹¹Yu-liang He and Hsiang-na Liu, *J. Phys. (Paris) Colloq.* **42**, C4-831 (1981).

¹²Z. Iqbal and S. Vepřek, *J. Phys. C* **15**, 377 (1982).

¹³Z. Vardeny, T. X. Zhou, H. Stoddart, and J. Tauc, *Solid State Commun.* **65**, 1049 (1988).

¹⁴D. Monroe, *Phys. Rev. Lett.* **54**, 146 (1985).